16th Australasian Fluid Mechanics Conference
Crowne Plaza, Gold Coast, Australia
2-7 December 2007

A Numerical Model of an Electrostatic Precipitator

Shah M E Haque[1*], M G Rasul[2], M M K Khan[2], A V Deev[1], and N Subaschandar[1]

[1] Process Engineering & Light Metals (PELM) Centre,
Faculty of Sciences, Engineering and Health
Central Queensland University
Gladstone, Queensland 4680
AUSTRALIA

[2] College of Engineering and the Built Environment
Faculty of Sciences, Engineering and Health
Central Queensland University
Rockhampton, Queensland 4702
AUSTRALIA

Abstract

This paper presents a Computational Fluid Dynamics (CFD) model for a wire-plate electrostatic precipitator (ESP). The turbulent gas flow and the particle motion under electrostatic forces are modelled using the CFD code FLUENT. Numerical calculations for the gas flow are carried out by solving the Reynolds-averaged Navier-Stokes equations and turbulence is modelled using the k-ε turbulence model. An additional source term is added to the gas flow equation to capture the effect of electric field. This additional source term is obtained by solving a coupled system of the electric field and charge transport equations. The particle phase is simulated by using Discrete Phase Model (DPM). The results of the simulation are presented showing the particle trajectory inside the ESP under the influence of both aerodynamic and electrostatic forces. The simulated results have been validated by the established data. The model developed is useful to gain insight into the particle collection phenomena that takes place inside an industrial ESP.

Introduction

An accurate CFD model of an ESP plays an important role in performance optimization by predicting the flow field characteristics and particle trajectories inside the ESP. The plate-type ESP of the local power plant consists of a series of parallel collection plates, spaced 400 mm apart, oriented along the direction of the flue gas flow. A number of thin discharge electrodes (DE) hang vertically between these plates. The precipitation process involves charging particles of the flue gas by applying high negative voltage to the discharge electrodes and driving the charged particles towards the grounded collection electrodes (CE) by the electric field produced. The collected particles are then removed from the collection electrodes by rapping process. The negligible change of the electric field in the vertical direction justifies a two-dimensional approach of this study. Due to the symmetry between the plates, only half of the distance between the plates is considered for modeling purpose.

There is a limited research found in the literature on ESP simulation. Lami *et al.* [1], Zhao *et al.* [2], Park and Kim [3], Anagnostopoulos and Bergeles [4] simplified their simulation by modeling single wire configuration. Suda et al [5] included seven wires in their gas flow field model but considered only single wire segment for their ionic wind analysis. Single wire model might not capture the wake of the wires properly and it can not be assumed that the electric field or particle motions are recurrent in the gas flow direction. Hence three wires have been taken into consideration for this study to develop a representative numerical model of ESP. Only few studies [6, 7, 8] have been found in the literature where three wires have been considered for modeling ESP.

The present study attempts to develop a detailed numerical approach and a simulation procedure to predict the motion of gas, ions and particles inside an ESP channel. The simulated result has been verified with the available literature data. The two-dimensional Navier–Stokes equations have been used to model the gas flow. The particle motion is considered by means of Lagrangian approach.

Geometry Configuration

An ESP channel of the local power station consists of a series of discharge electrodes placed between two collecting electrodes having 400 mm spacing between them. Due to the symmetry of the geometry only half of a channel is modeled in this study as is shown in Figure 1. The Fluent Inc. geometry and mesh generation software "GAMBIT" was used as a preprocessor to create the geometry, discretize the fluid domain into small cells to form a volume mesh or grid and set up the appropriate boundary conditions. The computational mesh which consists of 15000 cells is shown in Figure 2.
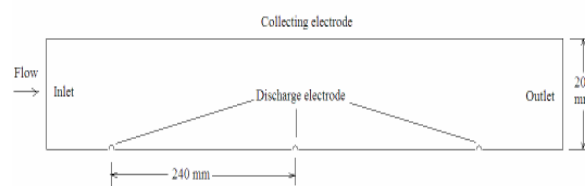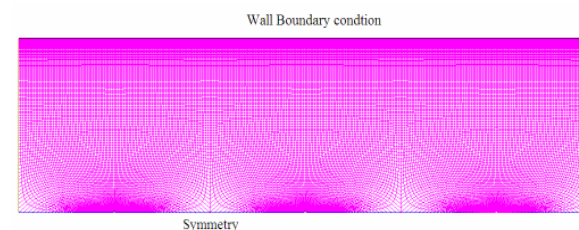

Figure 1. 2D geometry configuration

Figure 2. Computational mesh

1050

Numerical Model

Numerical calculations for the gas flow are carried out by solving the Reynolds-averaged Navier-Stokes equations. An additional source term is added to the gas flow equation to capture the effect of electric field. The particle phase is simulated by using Discrete Phase Model (DPM).

Gas Phase

The air inside the ESP is treated as incompressible Newtonian fluid due to the small pressure drop across the ESP. The flow can be described by the Conservation of mass equation [9]

$$\frac{\partial \rho}{\partial t} + \vec{\nabla} \cdot (\rho \vec{V}) = 0$$

(1)

and the Momentum equation known as Navier-Stokes equation [9]

$$\rho \vec{V} \cdot \vec{\nabla} \vec{V} = -\vec{\nabla} p + \mu \vec{\nabla}^2 \vec{V} + S$$

(2)

Where ρ is the fluid density (kg/m³), μ is the dynamic viscosity (kg/m/s) of the fluid, p is the fluid pressure (Pa) and $\vec{V}$ is the fluid velocity (m/s). S is the source term, which expresses the momentum force (N/m²) on the gas flow due to the electric field and can be expressed as [6]

$$S = \rho_{ion} \vec{E}$$

(3)

Where ρ_{ion} is the ion charge density (C/m³) and $\vec{E}$ is the electric field intensity (V/m).

Electrostatic Field

A high negative voltage is applied to the DE to generate the electrostatic field between the DE and the grounded CE. The electric field intensity $\vec{E}$ inside the ESP can described by the Gauss's law equation [10]

$$\nabla \cdot \vec{E} = \frac{\rho_{ion}}{\varepsilon_0}$$

(4)

Where

$$\vec{E} = -\nabla \phi$$

(5)

Combining Equations (3) and (4) gives the well known Poisson equation which is defined as

$$\nabla^2 \phi = -\frac{\rho_{ion}}{\varepsilon_0}$$

(6)

Where $\vec{E}$ is the electric field intensity (V/m), ϕ is the electric potential (Volt) and ε_0 is the permittivity of the free space. Under stationary conditions, the electrical flux density is divergence-free and can be written as [11].

$$\nabla \cdot \vec{J} = 0$$

(7)

Where $\vec{J}$ is the density of ionic current.

Assuming ion diffusion is of negligible importance compared to conduction [1, 11]), $\vec{J}$ can be expressed as

$$\vec{J} = \rho_{ion} b_{ion} \vec{E}$$

(8)

Where b_{ion} is the ion mobility.

Combining Equation (7) and (8) gives the following expression

$$\nabla \cdot (\rho_{ion} b_{ion} \nabla \phi) = 0$$

(9)

With the boundary conditions of Table 1 and an appropriate solution method, two transport variables ϕ and ρ_{ion} can be numerically calculated.

Particle Trajectory

FLUENT predicts the trajectory of a discrete phase particle (or droplet or bubble) by integrating the force balance on the particle, which is written in a Lagrangian reference frame. This force balance equates the particle inertia with the forces acting on the particle, and can be written as [12])

$$\frac{d\vec{u}_{p,i}}{dt} = F_D(\vec{u}_i - \vec{u}_{p,i}) + \frac{g_i(\rho_p - \rho)}{\rho_p} + \vec{F}_i$$

(10)

Where,

$$\frac{dx_i}{dt} = u \quad ; \quad i = x, y$$

(11)

Where ρ_p and $u_{p,i}$ denote particle density and velocity respectively. $\vec{F}_i$ corresponds to external forces exerted on the particle that, in the present study, are the electrostatic forces:

$$\vec{F}_i = \frac{\vec{E}_i q_p}{m_p}$$

(12)

Where $\vec{E}_i$ is the electric field intensities (V/m), q_p and m_p denote the electric charge (C) and mass (kg) of the particle respectively.

$F_D(\vec{u}_i - \vec{u}_{p,i})$ is the drag force per unit particle mass, where

$$F_D = \frac{3\mu C_D \, \mathrm{Re}}{4\rho_p d_p^2}$$

(13)

Here, $\vec{u}_i$ is the fluid phase velocity (m/s), μ is the molecular viscosity of the fluid (N.m/s), ρ is the fluid density (kg/m³) and $u_{p,i}, d_p$ and ρ_p denote the velocity (m/s), diameter (m) and density (kg/m³) of the particle respectively. Re is the relative Reynolds number, which is defined as

$$\mathrm{Re} \equiv \frac{\rho d_p |\vec{u}_{p,i} - \vec{u}_i|}{\mu}$$

(14)

The drag coefficient C_D can be calculated from the following equation [13]:

$$C_D = \frac{24}{\mathrm{Re}}(1 + b_1 \, \mathrm{Re}^{\, b_2}) + \frac{b_3 \, \mathrm{Re}}{b_4 + \mathrm{Re}}$$

(15)

Where

$$b_1 = \exp(2.3288 - 6.4581\phi + 2.4486\phi^2)$$
$$b_2 = 0.0964 + 0.5565\phi$$
$$b_3 = \exp(4.905 - 13.8944\phi + 18.4222\phi^2 - 10.2599\phi^3)$$
$$b_4 = \exp(1.4681 + 12.2584\phi - 20.7322\phi^2 + 15.8855\phi^3)$$

(16)

The shape factor, ϕ, is defined as

$$\phi = \frac{s}{S}$$

(17)

Where s is the surface area of a sphere having the same volume as the particle, and S is the actual surface area of the particle. The Reynolds number Re is computed with the diameter of a sphere having the same volume.

Particle Charge

The charge, q_p, which is acquired by a spherical dielectric particle with radius r_p and relative permittivity ε_r exposed to an ion flux in a field E can be calculated in the Lagrangian framework by the following Pauthenier equation [14, 15]):

$$q_p = [1 + 2(\frac{\varepsilon_r - 1}{\varepsilon_r + 1})]4\pi r_p^2 \varepsilon_0 |\vec{E}| \frac{t}{(t+\tau)}$$

(18)

Where ε_r is the relative permittivity of the gas, t is the resident time of the particle and τ is the charging time constant which can be defined by the following expression

$$\tau = \frac{4E}{J}$$

(19)

Computational Procedures

The finite volume methods have been used to discretize the partial differential equations of the model using the simplec method for pressure–velocity coupling and the second order upwind scheme to interpolate the variables on the surface of the control volume. The segregated solution algorithm was selected to solve the governing equations sequentially (i.e., segregated from one another). Standard wall functions, which are a collection of semi-empirical formulas and functions, were applied to bridge the viscosity-affected region between the wall and the fully-turbulent region. The wall function approach is a popular and practical option for the near-wall treatments for industrial flow simulations [12].

The electric potential on the discharge electrode surface is constant and equal to the corona onset value, whereas at the grounded collecting plates, its value is zero. At corona electrode electric potential Φ = 70 kV.

The charge density ρ_0 at the discharge electrode can be approximately calculated by [15]:

$$\rho_0 = -\frac{\varepsilon(E - E_0)}{ds}$$

(20)

Where E is the field strength in the cell adjacent to the emitting electrode, ds is the distance between the cell and the electrode surface. The corona onset field E_0 along the corona-emitting surface is assumed constant, which can be obtained according to Peek's law [16]:

$$E_o = E_{Peek} = 3.1X10^6 \delta(C_1 + C_2/\sqrt{\delta r})$$

(21)

Where E_{Peek} is the ion current threshold value for an electrode of radius r and C_1 = 1 V/m and C_2 = .031 V/√m in air of relative density δ with respect to the normal temperature and pressure conditions.

By solving Poisson's equation and the charge density equation alternatively and updating the boundary condition for ρ_0, the convergent solution for electric field and space charge density can be obtained.

The operating gas was ambient air while the particles were assumed to be ash with density equal to 600 kg/m^3. The particles of diameter equal to 2.0 μm were injected from the inlet surface with 0.0001 kg/s mass flow rate. Turbulent intensity at the inlet was 5%. Boundary conditions used to solve this problem are summarized in Table 1.

Table 1. Boundary conditions applied to the ESP model

	Gas velocity	Electric potential	Ion charge density	Particle motion
Inlet	$u_x = 1.0m/s$ $u_y = 0.0m/s$	$\nabla\phi = 0$	$\nabla\rho_{ion}$ = 0	$u_{p_x} = 1.0m/s$ $u_{p_y} = 0.0m/s$ Escape
Outlet	Mass conservation	$\nabla\phi = 0$	$\nabla\rho_{ion}$ = 0	Escape
Collecting electrode	No slip	$\phi = 0$	$\nabla\rho_{ion}$ = 0	Trap
Discharge electrode	No slip	$\phi = 70kV$	Peek law	Reflect

Result and Discussion

The numerical prediction is compared with the result of Choi and Fletcher [6] who developed their model considering 100 mm wire-plate distance rather than 200 mm distance. The predicted electric potential distribution along a line from the wire to the plate of this study yields a good agreement with their data up to a certain distance and then reaches zero potential at the collection electrode as shown in Figure 3. As stated earlier the model of this study has been developed according to the specification of the ESP used at a local power station. It is felt that the literature data [6] would have been the same as our predicted electric potential distribution data if their geometry had used 200 mm wire-plate distance.

Figure 4, 5 and 6 show the characteristic contours of the flow field. As expected, flow separation occurred after the discharge electrode which is shown in Figure 5.

Figure 7 shows the contours of the electric potential where the potential field forms an elliptical region around the discharge wires. Figure 8 shows the contours of ion charge density where an initial value of 10^{-7} C/m^3 is used on the surface of the discharge electrode [15].

It is found from Figure 9 that particles start to deviate from their straight path towards the collecting plates as they approach to the wires. As a result the DPM concentration is higher near the collection wall which is shown in Figure 10. DPM concentration distributions at the exit of the ESP are plotted in Figure 11 with and without consideration of the electrostatic field. The particle concentration near the collection wall is observed to be 14% higher in the presence of electrostatic field.
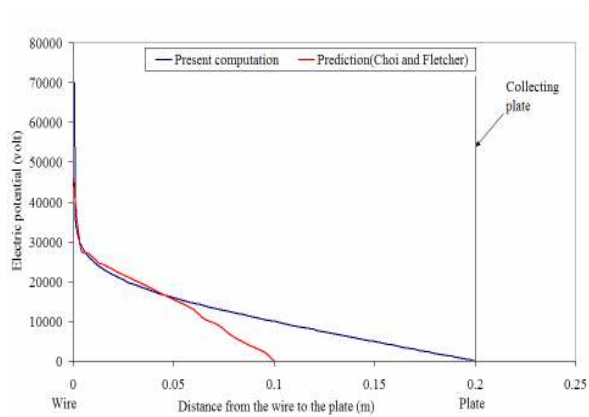
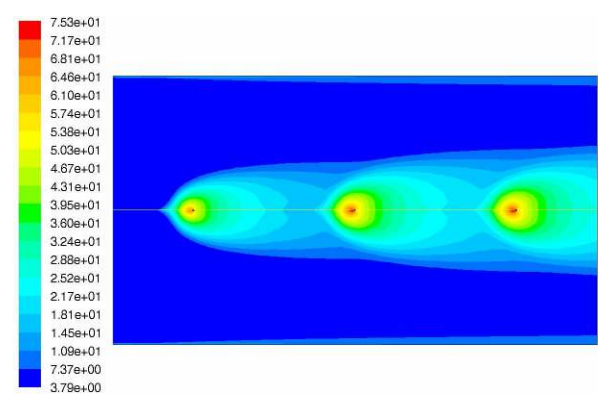Figure 3. Comparison with the published data

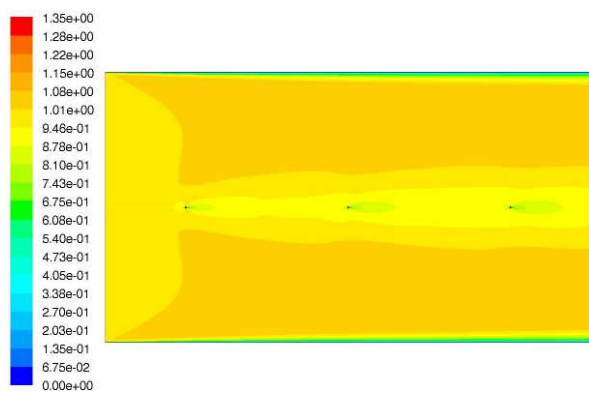Figure 6. Contours of turbulence intensity (%)

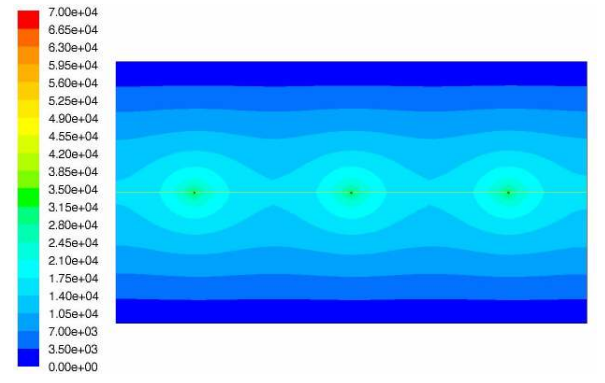
Figure 4. Contours of gas velocity magnitude (m/s)
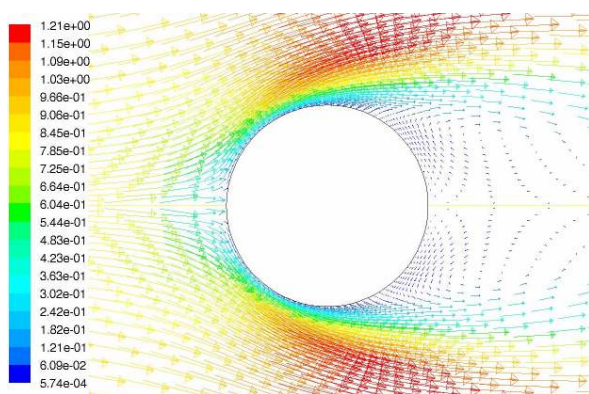

Figure 7. Contours of electric potential (Volt)
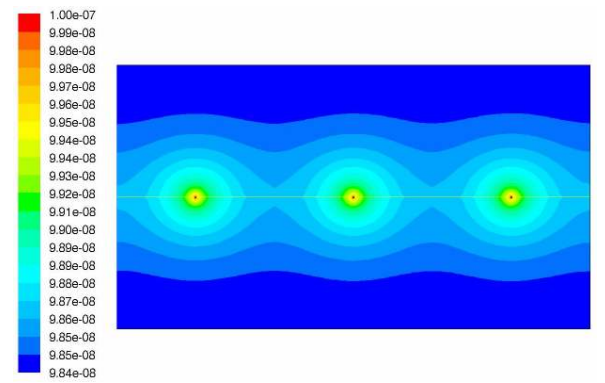

Figure 5. Velocity vectors of gas flow (m/s)

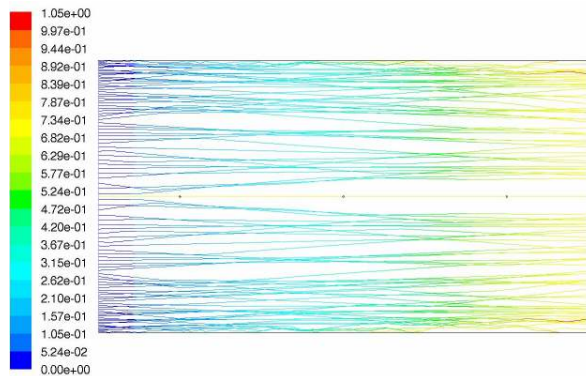Figure 8. Contours of ion charge density (C/m^3)
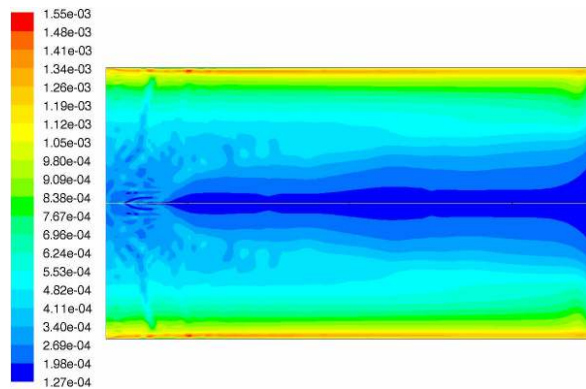
1053

Figure 9. Particle residence time (s)
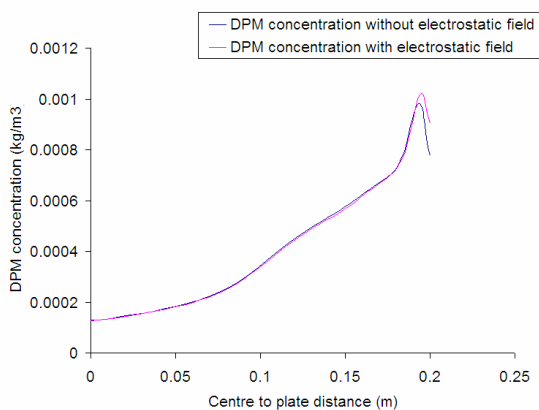

Figure 10. Contours of DPM concentration (kg/m^3)

Figure 11. DPM concentration distribution at exit

Concluding Remarks

A two dimensional numerical analysis for the ESP is presented. Realizable k-ε model for turbulence condition inside the ESP is applied. The electrostatic field is solved through writing and compiling a number of subroutines and linking them with the standard version of FLUNET 6.2 software. The DPM model is used to calculate the particle dynamics. Numerically predicted electric potential inside the ESP is compared with the literature data. The prediction is found in reasonable agreement with the literature data. The computational procedure developed can be applied to any geometrical and electrical configuration and can be useful in identifying options for improving performance of the industrial electrostatic precipitator.

References

[1] Lami, E., Mattachini, F., Gallimberti, I., Turri, R. and Tromboni, U., A numerical procedure for computing the voltage-current characteristics in electrostatic precipitator configurations, Journal of Electrostatics, 34, 1995, 385 – 399.

[2] Zhao, L., Cruz, E. Dela., Adamiak, K., Berezin, A. A., Chang, J.S. (2006). A numerical model of a wire-plate electrostatic precipitator under electrohydrodynamic flow conditions, The 10th International conference on electrostatic precipitator, Australia. 2006.

[3] Park, Seok. Joo & Kim, Sang. Soo., Effects of electrohydrodynamic flow and turbulent diffusion on collection efficiency of an electrostatic precipitator with cavity walls, Aerosol Science and Technology, 37, 2003, 574–586.

[4] Anagnostopoulos, J. & Bergeles, J., Corona discharge simulation in wire-duct electrostatic precipitator, Journal of Electrostatics 54, 2002, 129–147.

[5] Suda, J. M., Ivancsy, T., Kiss, I. and Berta, I., Complex analysis of ionic wind in ESP modeling, The 10th International conference on electrostatic precipitator, Australia. 2006.

[6] Choi, B.S., and Fletcher, C.A.J, Turbulent particle dispersion in an electrostatic precipitator, Applied mathematical modeling, 22, 1998, 1009 – 1021.

[7] Nikas, K.S.P., Varonos, A.A. and Bergeles, G.C., Numerical simulation of the flow and the collection mechanisms inside a laboratory scale electrostatic precipitator, Journal of electrostatics, 63, 2005, 423 – 443.

[8] Egli, Walter., Kogelschatz, Ulrich., Gerteisen, Edgar. A. and Gruber, Ralf., 3D computation of corona, ion induced secondary flows and particle motion in technical ESP configurations, Journal of electrostatic, 40&41, 1997, 425 – 430.

[9] Munson, B.R., Young, D.F., Okiishi, T.H., Fundamentals of fluid mechanics, 4th ed., John Wiley & Sons Inc., NY, 2002.

[10] Kallio, Gregory A. and Stock, David E., Computation of electrical conditions inside wire-duct electrostatic precipitators using a combined finite-element, finite-differnece technique, Journal of Applied Physics, 59 (6), 1986, 1799 – 1806.

[11] Poppner, Marc., Sonnenschin, Rainer. and Meyer, Jorg., Electric fields coupled with ion space charge. Part 2: computation, Journal of electrostatics, 63, 2005, 781 – 787.

[12] Fluent Inc. (2005). Fluent 6.2 User's Guide.

[13] Haider, A. and Levenspiel, O., Drag coefficient and terminal velocity of spherical and nonspherical particles. Powder Technology, 58, 1989, 63-70.

[14] Bottner, C.U. and Sommerfeld, M. (2001). Euler/Lagrange calculations of particle motion in turbulent flow coupled with an electric field. Proceedings of ECCOMAS Computational Fluid Dynamics Conference, 2001.

[15] Ye, Q. and Domnick, J., On the simulation of space charge in electrostatic powder coating with a corona spray gun, Powder technology, 135-136, 2003, 250 – 260.

[16] Peek, F.W., Determination Phenomena in High Voltage Engineering, McGraw-Hill, New York, 1929, 52–80.